

Contents lists available at ScienceDirect

Journal of the Mechanics and Physics of Solids

journal homepage: www.elsevier.com/locate/jmps



Modulated phononic crystals: Non-reciprocal wave propagation and Willis materials



H. Nassar^a, X.C. Xu^a, A.N. Norris^b, G.L. Huang^{a,*}

- ^a Department of Mechanical and Aerospace Engineering, University of Missouri, Columbia, MO 65211, USA
- ^b Mechanical and Aerospace Engineering, Rutgers University, Piscataway, NJ 08854-8058, USA

ARTICLE INFO

Article history: Received 9 December 2016 Revised 18 January 2017 Accepted 19 January 2017 Available online 23 January 2017

ABSTRACT

Research on breaking time-reversal symmetry in wave phenomena is a growing area of interest in the field of phononic crystals and metamaterials aiming to realize one-way propagation devices which have many potential technological applications. Here we investigate wave propagation in phononic crystals, periodic laminates in particular, where both elastic moduli and mass density are modulated in space and time in a wave-like fashion. The modulation introduces a bias which breaks time-reversal symmetry and reciprocity. A full characterization of how the dispersion curve transforms due to wave-like modulations is given in analytical and geometrical terms for both low (subsonic) and high (supersonic) modulation speeds. Theoretical findings are supported by numerical simulations. More specific to low frequencies, the macroscopic constitutive law of 1, 2 and 3D modulated laminates is proven to be of the Willis type with a non-negligible Willis coupling in the strictly scale-separated homogenization limit. The existence of a macroscopic stress-velocity and momentum-strain Willis coupling is in fact directly related to the breaking of reciprocity. Finally, closed form expressions of the macroscopic constitutive parameters are obtained and some elementary yet insightful energy bounds are derived and discussed.

© 2017 Elsevier Ltd. All rights reserved.

1. Introduction

The transformation method introduced by Greenleaf et al. (2003a, 2003b), and later by Leonhardt (2006) and Pendry et al. (2006), provided an efficient route to cloaking devices for phenomena governed by equations that are form-invariant by coordinate transformations such as the conductivity equation, the acoustic wave equation and Maxwell's equations of electromagnetism. As for elasticity, Milton et al. (2006) demonstrated that the equations of infinitesimal elastodynamics are invariant if written in a modified form due to Willis (1997). Unlike the usual elasticity equations, the Willis model allows for velocity-generated stresses and for strain-generated momenta through a constitutive law featuring stress-velocity and momentum-strain couplings, hereafter called Willis couplings.

Originating from considerations on elastic wave propagation in random matrix-inclusion composites (Willis, 1980a, 1980b), the Willis theory of elastodynamic homogenization regained attention in recent years due to the increasing interest in metamaterials and in their modelling on the macroscopic scale (see, e.g., Amirkhizi and Nemat-Nasser, 2008; Milton, 2007; Nassar et al., 2015; Nemat-Nasser and Srivastava, 2011; Norris et al., 2012; Shuvalov et al., 2011; Torrent et al., 2015).

E-mail address: huangg@missouri.edu (G.L. Huang).

^{*} Corresponding author.

Nonetheless, the use of the Willis model in the design of cloaking devices, or other wave-control devices and metamaterials in general, remains virtually nonexistent. In fact, one major obstacle is the inherent complexity of the Willis constitutive law due to non-locality and non-uniqueness issues (Willis, 2012). More fundamentally, the effective behaviour of elastic composites in the homogenization limit usually exhibits infinitesimally small Willis couplings and microstructures with substantial Willis couplings potentially useful in cloaking applications are yet to be found.

The purpose of the present paper is to characterize wave propagation in novel elastic media, time-modulated phononic crystals, and to show that their macroscopic constitutive behaviour in the rigorous homogenization low-frequency limit is of the Willis type with non-negligible Willis couplings. The considered media have elastic moduli and mass density that are modulated in space and in time in a wave-like fashion at a constant speed. The modulation introduces a bias which breaks time-reversal symmetry and reciprocity and manifests on the macroscopic scale through a Willis coupling.

In a conventional reciprocal medium with time-reversal symmetry, waves travelling in opposite directions necessarily have similar characteristics regarding phase and group velocities, dispersion and damping. Thus, breaking reciprocity can help control waves in novel and revolutionary ways by achieving selective one-way wave propagation (Fleury et al., 2014), directional mode conversion (Yu and Fan, 2009; Zanjani et al., 2015, 2014) and directional bandgaps (Swinteck et al., 2015; Trainiti and Ruzzene, 2016).

To break time-reversal symmetry, one of two classes of non-conventional topologies have to be adopted. Systems of the first class qualify as intrinsic and involve using structural chirality, dissipation and non-linearity (Liang et al., 2009; Liu et al., 2011, 2012; Mousavi et al., 2015). Systems of the second class are extrinsic as they are subjected to external stimuli in the form of a "pump wave" effectively modulating the properties of the host medium (Fleury et al., 2014; Yu and Fan, 2009) in both space and time. In practice, a time-modulation of stiffness can be induced by means of the photo-elastic effect (Gump et al., 2004; Swinteck et al., 2015) or by using programmable piezoelectric components (Casadei et al., 2012; Chen et al., 2016; 2014). On the other hand, mixed stiffness and mass density modulations are possible in magnetorheological elastomers (Danas et al., 2012) and in other soft non-linear media by controlled propagation of sonic booms for instance as suggested by Reed et al. (2003). The effects of wave-like modulations of constitutive parameters on wave propagation were investigated in earlier works on parametric amplification by many authors (see, e.g., Cassedy and Oliner, 1963a, 1963b; Hessel and Oliner, 1961; Simon, 1960; Slater, 1958) but only recently has the potential for directional wave control been recognized.

As for homogenization aspects, it seems that A.K.Lurie and collaborators were among the first to systematically study the macroscopic response of modulated phononic crystals that they called "dynamic materials". See the book by Lurie (2007) and references therein. Here, we extend their results to modulations of arbitrary profiles and to higher spatial dimensions while making explicit connections with Willis theory and non-reciprocity.

The paper proceeds as follows. Section 2 is an extensive case study of one-dimensional (1D) laminates where both mass-density and elastic stiffness are periodically modulated in a wave-like fashion. A dispersion equation is derived under the most general possible modulation configurations. The effects of the modulation are qualitatively and quantitatively characterized and illustrated in both high- and low-frequency regimes and also for subsonic and supersonic modulation speeds. In particular, a criterion for the opening of directional bandgaps in arbitrary low-contrast media is formulated. Furthermore, it is demonstrated that modulating either mass density or the elastic stiffness has only high-frequency repercussions on the location of bandgaps whereas modulating both of them effectively breaks reciprocity at low frequencies as well, thus generating a Willis coupling. Some anomalous transient responses highlighting the breaking of time-reversal symmetry are numerically simulated and illustrated.

In Section 3, the 1D analysis of Section 2 is generalized to higher dimensions. A closed form analytical expression of the macroscopic constitutive law of periodically modulated laminates in *d* dimensions is obtained in the homogenization limit. The macroscopic behaviour corresponds to a unique local Willis medium with non-negligible coupling tensors. Last, the Willis coupling tensors are explicitly calculated for slowly modulated isotropic layers.

Various elementary bounds on energy are derived and exploited in Section 4. In particular, sufficient conditions for the positive-definiteness of the macroscopic elastic stiffness tensor and of the macroscopic mass density tensor are presented. Finally, a few conclusions are drawn.

2. Wave propagation in 1D modulated phononic crystals

We start by investigating the effects of space-time modulations of stiffness and mass density on free wave propagation in 1D phononic crystals. The dispersion relation is derived and a geometric interpretation of the influence of modulations, in relation to non-reciprocity in particular, is provided and discussed for high- and low-frequency propagating waves. Finally, we establish a connection between acoustic non-reciprocity and a family of macroscopic constitutive behaviours exhibiting a Willis coupling.

2.1. Governing equations

For a 1D elastic medium, the constitutive and motion equations, in terms of the stress σ and the particle velocity v, are

$$\partial_x \nu = \partial_t (\sigma/\kappa), \quad \partial_x \sigma = \partial_t (\rho \nu),$$
 (1)

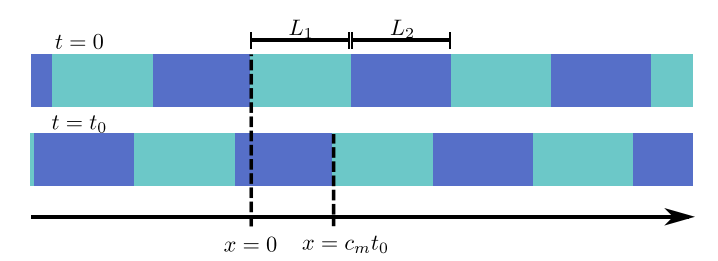


Fig. 1. A 1D two-phase modulated laminate sketched at two instants of time.

and can be expressed succinctly as

$$\partial_{x} \boldsymbol{\eta} + \partial_{t} (\boldsymbol{A} \boldsymbol{\eta}) = 0, \tag{2}$$

with

$$\boldsymbol{\eta} = \begin{bmatrix} \boldsymbol{v} \\ -\boldsymbol{\sigma} \end{bmatrix}, \quad \boldsymbol{A} = \begin{bmatrix} 0 & 1/\kappa \\ \rho & 0 \end{bmatrix}. \tag{3}$$

Elastic stiffness and mass density are designated by κ and ρ , respectively.

Energy conservation is a direct consequence of the governing equations. For passive materials featuring no sources (nor sinks), Eq. (1) implies the conservation equation

$$\partial_t \mathscr{E} - \partial_x (v\sigma) = 0.$$

where $\mathscr{E} = \frac{1}{2}\rho v^2 + \frac{1}{2}\kappa^{-1}\sigma^2$ and $-v\sigma$ are energy density and energy flux. When a perturbation travels across the medium, the total potential and kinetic energy \mathscr{E} at a given point can only change by channelling to neighbouring points in the form of an energy flux $-v\sigma$. In the following, we intend to investigate wave propagation in a family of modulated materials where stiffness and mass density are varied with respect to space and time. Energy conservation equation then becomes

$$\partial_t \mathscr{E} - \partial_x (v\sigma) = \frac{1}{2} (\partial_t \kappa) \varepsilon^2 - \frac{1}{2} (\partial_t \rho) v^2,$$

where $\varepsilon = \sigma/\kappa$ is strain. Changing κ and ρ in space and time will effectively pump energy into or out of the medium and will ultimately influence the way waves propagate.

Hereafter, we tackle 1D periodic media where κ and ρ are modulated in space and time in a wave-like fashion:

$$\kappa = \kappa(x, t) = \kappa(x - c_m t), \quad \rho = \rho(x, t) = \rho(x - c_m t),$$

with c_m being the modulation speed. Calling L the thickness of a unit cell, κ and ρ are L-periodic functions of x and of $x-c_mt$ and L/c_m -periodic functions of t. Beyond energy conservation, the wave nature of the modulation introduces a bias in space-time and breaks time-reversal symmetry: in general, when the medium supports a wave v(x, t), it will not support v(x, -t).

Wave propagation in one dimension depends upon the two derived parameters: phase velocity and impedance,

$$C = \sqrt{\kappa/\rho}, \quad Z = \sqrt{\rho\kappa},$$
 (4)

respectively. When c_m takes on values between the minimum and the maximum phase velocity, discontinuities in the travelling wave, reminiscent of sonic booms, may appear and invalidate the implicit smoothness hypotheses made throughout the paper. Further details can be found in the papers by Cassedy and Oliner (1963a, 1963b). Thus, in the following, it is understood that the modulation speed satisfies

$$(\forall \xi \in (0, L), \quad c(\xi) > |c_m|) \quad \text{or} \quad (\forall \xi \in (0, L), \quad c(\xi) < |c_m|), \tag{5}$$

which can be identified, respectively, as subsonic and supersonic regimes.

We begin by deriving the dispersion relation for media with unit cells of arbitrary profiles, and then move on to consider applications to laminates composed of discrete phases, i.e., with piecewise constant functions κ and ρ . A two-phase laminate is depicted in Fig. 1. First however, we modify the governing equations into a form which can be analyzed by standard methods.

2.2. Equations in the moving frame

Since κ and ρ depend on (x, t) through a unique combination, $x - c_m t$, the medium is more conveniently described with a new variable ε introduced by the change of variable

$$(\xi, t) = (x - c_m t, t), \quad (\partial_x, \partial_t) = (\partial_{\xi}, -c_m \partial_{\xi} + \partial_t).$$

Hence, the governing Eq. (3) can be rewritten as

$$\partial_{\varepsilon}[(\mathbf{I}-c_{m}\mathbf{A})\boldsymbol{\eta}]+\mathbf{A}\partial_{t}\boldsymbol{\eta}=0,$$

where **A** now depends on ξ but not on t. Then, with the change of the state vector

$$\psi = (I - c_m A)\eta,$$

we obtain

$$\partial_{\varepsilon} \psi + \mathbf{B} \partial_{t} \psi = 0 \tag{6}$$

where the new constitutive matrix is

$$\mathbf{B} = \mathbf{A}(\mathbf{I} - c_m \mathbf{A})^{-1} = \frac{1}{c^2 - c_m^2} \begin{bmatrix} c_m & 1/\rho \\ \kappa & c_m \end{bmatrix}.$$

This is guaranteed to remain finite by virtue of the restrictions (5).

Note that the form of the Eq. (6) for the modified state vector ψ implies that it is continuous across interfaces. The continuity of the first component of ψ is equivalent to the continuity of the displacement u and is expected. The continuity of the second component of ψ is equivalent to that of the modified stress $\sigma + c_m \rho v$ and replaces the usual stress continuity hypothesis due to the presence of moving discontinuities in the constitutive parameters κ and ρ . The latter property can be proven by virtue of a "Reynolds transport theorem".

2.3. Dispersion relation

Since **B** is L-periodic in ξ , we can look for harmonic plane wave solutions

$$\psi(\xi,t) = \psi(\xi)e^{-i\Omega t},$$

subject to the Floquet-Bloch periodic boundary condition

$$\psi(\xi + L) = \psi(\xi)e^{iKL},\tag{7}$$

where wavenumber K and frequency Ω describe the phase of the travelling wave in the moving frame of reference (ξ, t) . The state vector thus satisfies

$$\psi(\xi) = \mathbf{M}(\xi, \xi_0) \psi(\xi_0),$$

where the matricant $M(\xi, \xi_0)$ (Pease, 1965) is the solution of the ordinary differential equation

$$\partial_{\xi} \mathbf{M} = i\Omega \mathbf{B}(\xi) \mathbf{M}, \quad \mathbf{M}(\xi_0, \xi_0) = \mathbf{I}.$$

The existence of a non-trivial solution ψ satisfying the Floquet–Bloch boundary condition (7) is therefore equivalent to the vanishing of the determinant

$$\det \left(\boldsymbol{M}(\boldsymbol{\xi} + \boldsymbol{L}, \boldsymbol{\xi}) - e^{iKL} \boldsymbol{I} \right) = 0.$$

Noting that \mathbf{B} has the form

$$\mathbf{B} = \frac{c_m}{c^2 - c_m^2} \mathbf{I} + \frac{c}{c^2 - c_m^2} \mathbf{J}, \quad \mathbf{J} = \begin{bmatrix} 0 & 1/z \\ z & 0 \end{bmatrix}$$

the matricant may be written

$$\boldsymbol{M}(\xi,\xi_0) = \exp\left(ic_m\Omega\int_{\xi_0}^{\xi}\frac{\mathrm{d}\xi}{c^2-c_m^2}\right)\!\!\boldsymbol{N}(\xi,\xi_0)$$

where the 2 \times 2 unitary matrix $N(\xi, \xi_0)$ is the solution of

$$\partial_{\xi} \mathbf{N} = \frac{i\Omega c}{c^2 - c_m^2} \mathbf{J} \mathbf{N}, \quad \mathbf{N}(\xi_0, \xi_0) = \mathbf{I}.$$

The Floquet-Bloch condition therefore reduces to

$$\cos\left(KL - \left(\frac{c_m \Omega L}{c^2 - c_m^2}\right)\right) = \frac{1}{2} \operatorname{tr} \mathbf{N}(\xi + L, \xi)$$
(8)

where the brackets $\langle \cdot \rangle = \frac{1}{l} \int_0^L d\xi$ denote the operator of averaging over a unit cell and tr is the trace operator.

Note finally that, as mentioned earlier, ψ has wavenumber K and frequency Ω in the moving frame of reference (ξ, t) . In the original frame (x, t), the travelling wave wavenumber k and temporal frequency ω can be retrieved based on

$$kx - \omega t = K\xi - \Omega t$$
.

from which it can be inferred that

$$k = K, \quad \omega = \Omega + c_m k.$$
 (9)

2.4. Discrete layering

Each phase in the unit cell, indexed with j from 1 to J, has stiffness κ_j , mass density ρ_j , phase velocity $c_j = \sqrt{\kappa_j/\rho_j}$, impedance $z_j = \sqrt{\rho_j \kappa_j}$ and a thickness L_j . In this setting, wave-like modulations alter the underlying microstructure by shifting the interfaces between phases (Fig. 1). Interfaces that were located at

$$x = nL + \sum_{m=1}^{j} L_m, \quad n \in \mathbb{Z}, \quad 1 \leq j \leq J,$$

are now moving at a constant speed c_m and, at instant t, are located at

$$x = nL + \sum_{m=1}^{j} L_m + c_m t, \quad n \in \mathbb{Z}, \quad 1 \le j \le J.$$

Over phase j, \boldsymbol{B} is a constant matrix \boldsymbol{B}_j so that the equation for \boldsymbol{N} is a linear first order ordinary differential equation with constant coefficients. Using the fact that $\boldsymbol{J}^2 = \boldsymbol{I}$ the matrix exponential solution, say across phase 1, $\boldsymbol{N}(L_1, 0)$ is simply

$$\mathbf{N}_{1} = \exp\left(i\frac{c_{m}\Omega L_{1}}{c_{1}^{2} - c_{m}^{2}}\mathbf{J}_{1}\right) = \cos\left(\frac{c_{1}\Omega L_{1}}{c_{1}^{2} - c_{m}^{2}}\right)\mathbf{I} + i\sin\left(\frac{c_{1}\Omega L_{1}}{c_{1}^{2} - c_{m}^{2}}\right)\mathbf{J}_{1}.$$
(10)

By induction over the I phases of the unit cell, we obtain

$$\mathbf{N}(L,0) = \prod_{i=1}^{J} \mathbf{N}_{j}.$$

As an example, for J=2 and upon calculating the product N_1N_2 , we retrieve the (k, ω) -dispersion relation of Lurie (2007)

$$\cos\left[kL - c_{m}(\omega - c_{m}k)\left(\frac{L_{1}}{c_{1}^{2} - c_{m}^{2}} + \frac{L_{2}}{c_{2}^{2} - c_{m}^{2}}\right)\right] \\
= \cos\left(\frac{\omega - c_{m}k}{c_{1}^{2} - c_{m}^{2}}c_{1}L_{1}\right)\cos\left(\frac{\omega - c_{m}k}{c_{2}^{2} - c_{m}^{2}}c_{2}L_{2}\right) - \frac{1}{2}\left(\frac{z_{1}}{z_{2}} + \frac{z_{2}}{z_{1}}\right)\sin\left(\frac{\omega - c_{m}k}{c_{1}^{2} - c_{m}^{2}}c_{1}L_{1}\right)\sin\left(\frac{\omega - c_{m}k}{c_{2}^{2} - c_{m}^{2}}c_{2}L_{2}\right). \tag{11}$$

For $c_m = 0$, the standard dispersion relation of a non-modulated two-phase phononic crystal is recovered:

$$\cos(kL) = \cos\left(\frac{\omega}{c_1}L_1\right)\cos\left(\frac{\omega}{c_2}L_2\right) - \frac{1}{2}\left(\frac{z_1}{z_2} + \frac{z_2}{z_1}\right)\sin\left(\frac{\omega}{c_1}L_1\right)\sin\left(\frac{\omega}{c_2}L_2\right). \tag{12}$$

It is important to emphasize that the derived dispersion relation (8) is valid for any number of layers J, for large or small mismatch between layers and for arbitrary modulation speeds c_m except these coinciding with phase velocity in any of the layers. Thus, in the context of discrete laminates, the assumption (5) becomes

$$|c_m| < \min c_i \quad \text{or} \quad |c_m| > \max c_i. \tag{13}$$

2.5. Acoustic non-reciprocity

By inspecting the dispersion relation (11), it becomes clear that, in general, if (k, ω) belongs to the dispersion curve, then $(-k, \omega)$ does not. The modulation speed c_m indeed breaks reciprocity, i.e., time reversal symmetry, so that waves travelling to the right and to the left have different characteristics, e.g., different group velocity, phase velocity or damping coefficient. In order to understand how time modulation transforms the dispersion relation, we first focus our attention on slow modulations and neglect effects related to c_m^n , for $n \ge 2$. This simplification remains valid as long as

$$|c_m| \ll \min c_i$$
.

Fast modulations are treated afterwards.

2.5.1. Slow modulations

To first order in c_m , the dispersion relation (11) can be approximated by

$$\cos\left[\left(k-c_{m}\omega\left\langle c^{-2}\right\rangle\right)L\right] = \cos\left(\frac{\omega-c_{m}k}{c_{1}}L_{1}\right)\cos\left(\frac{\omega-c_{m}k}{c_{2}}L_{2}\right) - \frac{1}{2}\left(\frac{z_{1}}{z_{2}} + \frac{z_{2}}{z_{1}}\right)\sin\left(\frac{\omega-c_{m}k}{c_{1}}L_{1}\right)\sin\left(\frac{\omega-c_{m}k}{c_{2}}L_{2}\right). \tag{14}$$

It is then clear that (k, ω) is a solution to (14) if and only if the transformed couple

$$T(k, \omega) = (k - c_m \omega \langle c^{-2} \rangle, \omega - c_m k),$$

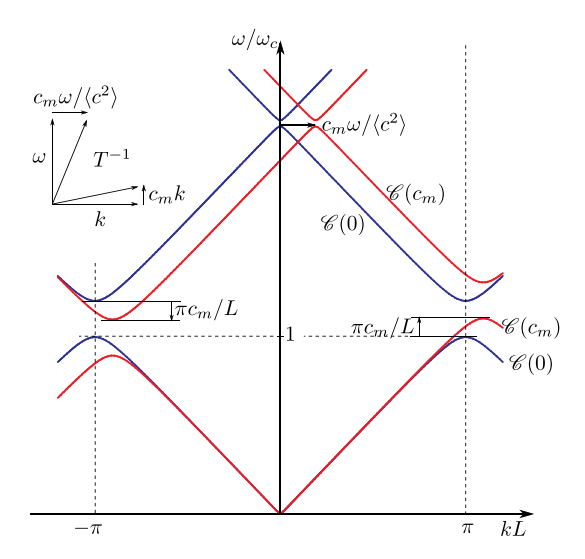


Fig. 2. The lower branches of a typical dispersion curve of a 1D phononic crystal: with ($\mathscr{C}(c_m)$, in red) and without ($\mathscr{C}(0)$, in blue) modulation. The shearing effect of T^{-1} is sketched. The corresponding phononic crystal has two phases with contrasts of $\kappa_1/\kappa_2 = 1.5$ and $\rho_1/\rho_2 = 1.2$. The modulation speed c_m is $\sqrt{\kappa_2/\rho_2}/10$. Wavenumbers and frequencies are respectively normalized with respect to the unit cell length L and to the first cut-off frequency in the absence of modulation ω_c . (For interpretation of the references to colour in this figure legend, the reader is referred to the web version of this article.)

is a solution to (12). Thus, calling $\mathscr{C}(c_m)$ the dispersion curve of the laminate modulated at speed c_m , we have, to first order in c_m ,

$$(k,\omega) \in \mathcal{C}(c_m) \iff T(k,\omega) \in \mathcal{C}(0),$$

where $\mathscr{C}(0)$ is the dispersion curve of the non-modulated laminate. In other words, to first order in c_m , the dispersion curve of the modulated laminate $\mathscr{C}(c_m)$ is obtained by uniformly shearing $\mathscr{C}(0)$ in the (k, ω) -space as dictated by the linear transformation T (Fig. 2). Furthermore, revisiting Eqs. (8) and (10) shows that the above characterization generalizes for any number of phases J, and indeed for any travelling modulation subject to the constraints (5). In conclusion, the dispersion curve of a 1D periodic medium modulated at speed c_m , $\mathscr{C}(c_m)$, can be deduced from the dispersion curve of the same medium in the absence of the modulation, $\mathscr{C}(0)$, according to

$$\mathscr{C}(c_m) = T^{-1}(\mathscr{C}(0))$$

As an application, consider the bandgaps located at the edges of the Brillouin zones $k = \pi n/L$, $n \in \mathbb{Z}\setminus\{0\}$. Due to the modulation, they all get shifted by an amount equal to $\pi nc_m/L$ (Fig. 2). Accordingly, total bandgaps, blocking right- and left-going waves, become directional bandgaps, blocking either right- or left-going waves, whenever the shift is larger than half of the gap width. Namely, the nth bandgap, of width $\Delta_n \omega$, becomes directional if

$$|c_m| \geq \frac{L\Delta_n\omega}{2\pi n}.$$

Hence, high-frequency bandgaps are the first to become directional whereas low-frequency bandgaps require higher modulation speeds. Note that the assumption made on the smallness of c_m makes the previous result valid in the limit

$$\frac{L\Delta_n\omega}{2\pi n}\ll\min c_j.$$

For instance, it holds at high enough frequencies (large n) and/or for low contrast materials (small $\Delta_n \omega$). In the latter case, the width of the nth bandgap is directly related to the amplitude of the impedance modulation. Calling $\Delta_n z$ the nth Fourier coefficient of z, the nth bandgap is directional if

$$|c_m| \geq \frac{\langle c \rangle}{n} \sqrt{\left|\frac{\Delta_n z}{\langle z \rangle}\right|}.$$

Slater (1958) and Cassedy and Oliner (1963a, 1963b), among others in the previous century, derived similar results for 1D low-contrast media where either κ or ρ is sinusoidally modulated. More recently, Swinteck et al. (2015) and Trainiti and Ruzzene (2016) reinterpreted these results in terms of directional bandgaps. The present considerations generalize earlier works to arbitrary 1D low-contrast phononic crystals where both κ and ρ are modulated in space and time.

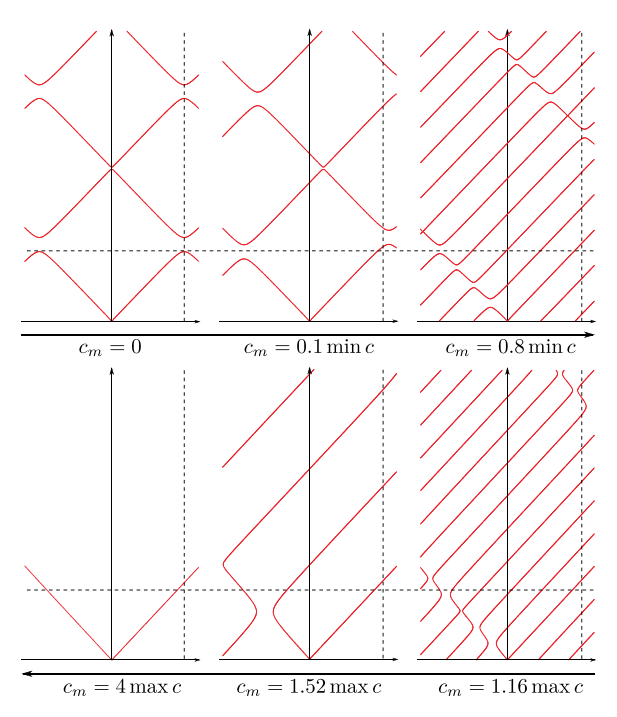


Fig. 3. The dispersion curve of a modulated two-phase laminate $(\kappa_1/\kappa_2 = 1.5, \rho_1/\rho_2 = 1.2)$ for increasing subsonic (top row) and supersonic (bottom row) modulation speeds c_m . Horizontal axis refer to kL and vertical axis to ω/ω_c . The dashed lines intersect at $kL = \pi$ and $\omega/\omega_c = 1$.

2.5.2. Fast modulations

By fast modulations, we mean those for which the modulation speed c_m is comparable to but lower than $\min c$ or greater than $\max c$ in accordance with inequality (13). Here, the influence of all orders of c_m needs be taken into account. To that purpose, we observe that the general dispersion relation (8) depends, when it comes to the constitutive properties, on the profiles of phase velocity c and impedance c. It is appropriate thus to rename c0(0, c0) the dispersion curve of the non-modulated medium and c0(c0, c0) that of the one modulated at c0. The transformation from the former to the latter happens in two steps.

First, according to Eq. (10), the curve $\mathscr{C}(0,c,z)$ is transformed into $\mathscr{C}(0,\hat{c},z)$ with¹

$$\hat{c} = |c - c_m/c^2|.$$

That is, when the modulation is turned on, it is as if the constitutive parameters (c, z) were changed into (\hat{c}, z) . The modified phase velocities are shifted downwards in the subsonic regime $(c_m < \min c)$ and upwards in the supersonic regime $(c_m > \max c)$. Hence, one expects bands to become "denser" around the edges of the sonic regime where phase velocities are the lowest (see Fig. 3).

Second, Eqs. (8) and (9) imply that $\mathscr{C}(c_m, c, z)$ is related to $\mathscr{C}(0, \hat{c}, z)$ through

$$(k,\omega) \in \mathscr{C}(c_m,c,z) \iff T(k,\omega) \in \mathscr{C}(0,\hat{c},z).$$

The transformation T has now the exact expression

$$T(k,\omega) = \left(k - c_m(\omega - c_m k) \left(\frac{1}{c^2 - c_m^2}\right), \omega - c_m k\right)$$

including all orders of c_m . In other words, the inverse transform T^{-1} finitely deforms $\mathscr{C}(0,\hat{c},z)$ into the dispersion curve of the modulated medium $\mathscr{C}(c_m,c,z)$. This deformation becomes so severe in the supersonic regime that some "horizontal" bandgaps become "vertical" (See Fig. 3). These vertical gaps indicate the existence of potentially unstable solutions with a real wavenumber and an imaginary frequency (Cassedy and Oliner, 1963a, 1963b).

Fig. 3 illustrates the change inflicted on the dispersion curve for various (positive) modulation speeds. The effect of slow modulations is to hybridize total bandgaps and create couples of directional gaps as mentioned earlier. This is seen by comparing the dispersion diagrams plotted for $c_m = 0$ and $c_m = 0.1 \, \text{min} \, c$. For faster modulations ($c_m \to (\text{min} \, c)^-$), directionality

¹ Absolute values are added here to ensure positivity of phase velocity and ease interpretations. In fact, when $c - c_m^2/c$ changes signs, matrix N transforms into its Hermitian conjugate N^* which, in fine, does not alter the dispersion relation.

in wave propagation can be observed at low frequencies: when the modulation speed is positive, i.e., the modulation is travelling to the right, left-going waves are often blocked whereas right-going waves are always transmitted.

Finally, remark that the constitutive parameters of the phononic crystal change in time with a frequency $2\pi c_m/L$ and in space with a frequency $2\pi/L$. Consequently, for infinitely fast modulations, these parameters are effectively being changed in time only and at an infinitely high frequency $2\pi c_m/L \gg \omega$. In this extreme setting, a travelling wave effectively sees the parameters of the laminate homogenized in time. Therefore, the medium behaves as if it had an effective mass density equal to the harmonic mean of densities and an effective stiffness equal to the arithmetic mean of stiffnesses (e.g., plot $c_m = 4(\max c)$ on Fig. 3). The resulting dispersion relation is

$$\langle \kappa \rangle k^2 - \frac{\omega^2}{\langle 1/\rho \rangle} = 0.$$

Wave propagation within such a phononic crystal is both dispersionless and reciprocal.

2.6. Homogenization

For low frequencies, when the wavelength of propagating elastic waves is much larger than the characteristic size of the microstructure, the properties of the phononic crystal can be well described using homogenized parameters or effective medium parameters. Effective medium theory has been successful in modelling many unconventional wave phenomena in metamaterials.

2.6.1. Slow modulations

It is well known that the dispersion relation of a non-modulated phononic crystal at low frequencies, i.e., in the homogenization limit, reduces to

$$\frac{1}{\langle 1/\kappa \rangle} k^2 - \langle \rho \rangle \omega^2 = 0. \tag{15}$$

The general results of the previous subsection imply that the dispersion curve of the same phononic crystal when slowly modulated at speed c_m is

$$\frac{1}{\langle 1/\kappa \rangle} (k - c_m \omega \langle c^{-2} \rangle)^2 - \langle \rho \rangle (\omega - c_m k)^2 = 0.$$

By expanding, regrouping and neglecting higher powers of c_m , one gets

$$\frac{1}{\langle 1/\kappa \rangle} k^2 + 2c_m \left(\langle \rho \rangle - \frac{\langle c^{-2} \rangle}{\langle 1/\kappa \rangle} \right) \omega k - \langle \rho \rangle \omega^2 = 0,$$

or, inserting $c^2 = \kappa/\rho$,

$$\frac{1}{\langle 1/\kappa \rangle} k^2 + 2c_m \langle \rho \rangle \left(1 - \frac{\langle \rho/\kappa \rangle}{\langle \rho \rangle \langle 1/\kappa \rangle} \right) \omega k - \langle \rho \rangle \omega^2 = 0.$$

Consequently, the phase/group velocity $V = \omega/k$ of low-frequency waves travelling in the modulated phononic crystal satisfies

$$\frac{1}{\langle 1/\kappa \rangle} + 2c_m \langle \rho \rangle \left(1 - \frac{\langle \rho/\kappa \rangle}{\langle \rho \rangle \langle 1/\kappa \rangle} \right) V - \langle \rho \rangle V^2 = 0.$$

In the absence of modulation ($c_m = 0$), the previous equation has two roots of equal value and opposite sign

$$V = \pm \frac{1}{\sqrt{\langle \rho \rangle \langle 1/\kappa \rangle}}$$

attributed to left-going and right-going waves. However, in the presence of even a slow modulation, the two roots become

$$V = \left(1 - \frac{\langle \rho/\kappa \rangle}{\langle \rho \rangle \langle 1/\kappa \rangle}\right) c_m \pm \frac{1}{\sqrt{\langle \rho \rangle \langle 1/\kappa \rangle}}$$

so that left-going and right-going waves now travel at different group velocities, breaking thus time-reversal symmetry at low frequencies. This is illustrated on Fig. 4 where the dispersion diagram is asymmetric even when restricted to the range $\omega/\omega_c\ll 1$ where ω_c is the first cut-off frequency of the non-modulated phononic crystal. The non-dimensional constitutive parameter

$$\beta = 1 - \frac{\langle \rho/\kappa \rangle}{\langle \rho \rangle \langle 1/\kappa \rangle} = 1 - \frac{\langle 1/c^2 \rangle}{\langle z/c \rangle \langle 1/(zc) \rangle}$$

² The homogenization limit is dispersionless.

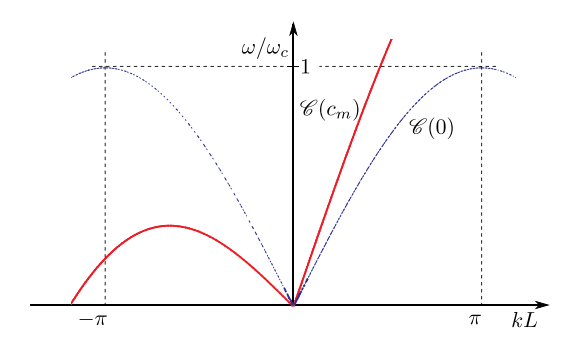


Fig. 4. The dispersion curve of a 1D laminate: with $(\mathscr{C}(c_m), in red solid lines)$ and without $(\mathscr{C}(0), in blue dotted lines)$ modulation when the frequency is within the homogenization limit. The corresponding laminate has two phases with high contrasts of $\kappa_1/\kappa_2 = \rho_1/\rho_2 = 100$ in order to maximize non-reciprocity. The modulation speed c_m is c/10. (For interpretation of the references to colour in this figure legend, the reader is referred to the web version of this article.)

can be seen as a measure of contrast and of non-reciprocity at low frequencies. Note that it vanishes if either κ or ρ is uniform. As a result, these low-frequency effects were missed by earlier papers where either κ or ρ is modulated but not the other.

The defined contrast parameter β can be either positive or negative. When β is positive, waves travelling with the modulation are accelerated and waves travelling in the opposite direction of the modulation are decelerated. This happens for instance when c is uniform across phases so that

$$\beta = 1 - \frac{1}{\langle z \rangle \langle 1/z \rangle} \ge 0.$$

Conversely, when β is negative, waves travelling along the modulation are decelerated and waves going in the inverse direction are accelerated. Such phenomena can be observed in medium with a uniform z in which case

$$\beta = 1 - \frac{\left\langle 1/c^2 \right\rangle}{\left\langle 1/c \right\rangle^2} \le 0.$$

In terms of a macroscopic equation of motion, the wave travelling in the modulated laminate in the low-frequency limit, hereafter called U, is governed by

$$\frac{1}{\langle 1/\kappa \rangle} \partial_x^2 U + 2c_m \left(\frac{\langle \rho/\kappa \rangle}{\langle 1/\kappa \rangle} - \langle \rho \rangle \right) \partial_x \partial_t U - \langle \rho \rangle \partial_t^2 U = 0.$$

This equation of motion is of Willis (1997) type:

$$\kappa^e \partial_x^2 U + 2s \partial_x \partial_t U - \rho^e \partial_t^2 U = 0.$$

Parameter κ^e is interpreted as a macroscopic stiffness, ρ^e as a macroscopic mass density and s as a coupling coefficient with the dimension of an impedance. The existence of a mixed derivative term $\partial_x \partial_t U$ implies that, on the level of the constitutive behaviour, the macroscopic stress is coupled to the macroscopic velocity and the macroscopic momentum is coupled to the macroscopic strain, the coupling being as strong as the non-reciprocity itself.

Effective constitutive behaviours of the Willis type are usually obtained by micromechanical homogenization approaches for relatively high frequencies and, as frequency decreases, reduce to standard constitutive behaviours where the mentioned coupling vanishes (Nassar et al., 2016; Shuvalov et al., 2011; Willis, 1997). For the modulated medium under consideration however, the coupling does not vanish at low frequencies. In the next section, a generalization to faster modulations is presented.

2.6.2. Fast modulations

When c_m takes finite values, applying the two-step transformation described in Section 2.5.2 to the macroscopic dispersion Eq. (15) of a non-modulated medium leads again to a Willis type equation of motion. The macroscopic constitutive parameters now have the expressions

$$\begin{split} \kappa^e &= \left\langle \frac{\kappa}{\kappa - c_m^2 \rho} \right\rangle^2 \left\langle \frac{1}{\kappa - c_m^2 \rho} \right\rangle^{-1} - c_m^2 \left\langle \frac{\rho \kappa}{\kappa - c_m^2 \rho} \right\rangle, \\ \rho^e &= -c_m^2 \left\langle \frac{\rho}{\kappa - c_m^2 \rho} \right\rangle^2 \left\langle \frac{1}{\kappa - c_m^2 \rho} \right\rangle^{-1} + \left\langle \frac{\rho \kappa}{\kappa - c_m^2 \rho} \right\rangle, \\ s &= c_m \left\langle \frac{\kappa}{\kappa - c_m^2 \rho} \right\rangle \left\langle \frac{\rho}{\kappa - c_m^2 \rho} \right\rangle \left\langle \frac{1}{\kappa - c_m^2 \rho} \right\rangle^{-1} - c_m \left\langle \frac{\rho \kappa}{\kappa - c_m^2 \rho} \right\rangle. \end{split}$$

As for the macroscopic phase/group velocity, it is a solution to the equation

$$\kappa^e - 2sV - \rho^e V^2 = 0.$$

Thus, as a function of the macroscopic constitutive parameters, it reads

$$V = \left(-s \pm \sqrt{s^2 + \rho^e \kappa^e}\right) / \rho^e,$$

or,

$$V = c_m + \left(\left\langle\frac{c_m}{c^2 - c_m^2}\right\rangle \pm \sqrt{\left\langle\frac{c/z}{c^2 - c_m^2}\right\rangle \left\langle\frac{cz}{c^2 - c_m^2}\right\rangle}\right)^{-1},$$

as a function of the microscopic impedance z, phase velocity c and modulation speed c_m . In the foregoing expression, the denominator $c^2 - c_m^2$ remains positive (resp. negative) across the whole unit cell in the subsonic (resp. supersonic) regime. Consequently, macroscopic phase velocities are always real valued which is equivalent to the positivity of the discriminant

$$s^2 + \rho^e \kappa^e > 0$$
.

This property is a particular case of a more general one proven in Section 4.3. Nonetheless, at some supersonic modulation speeds, group velocity can become infinite suggesting that V is different than the necessarily bounded energy velocity. In fact, energy arrival cannot precede that of the wave front which propagates across large distances at the always finite velocity³

$$V_f = \left\langle \frac{1}{\pm c - c_m} \right\rangle^{-1} + c_m.$$

2.6.3. Example: effective properties of a medium with uniform phase velocity

To illustrate the macroscopic behaviour of a 1D modulated laminate in a simple context, we assume in this subsection that c is uniform across the unit cell so that only the impedance z is modulated. The effective parameters then become

$$\kappa^{e} = \frac{c}{c^{2} - c_{m}^{2}} \left(c^{2} \langle 1/z \rangle^{-1} - c_{m}^{2} \langle z \rangle \right),$$

$$\rho^{e} = \frac{1/c}{c^{2} - c_{m}^{2}} \left(-c_{m}^{2} \langle 1/z \rangle^{-1} + c^{2} \langle z \rangle \right),$$

$$s = \frac{c_{m}c}{c^{2} - c_{m}^{2}} \left(\langle 1/z \rangle^{-1} - \langle z \rangle \right),$$

and the macroscopic phase velocity simplifies into

$$V = c_m + \frac{c^2 - c_m^2}{c_m \pm c\sqrt{\langle 1/z \rangle \langle z \rangle}},$$

whereas the wave front velocity V_f becomes a constant equal to c as expected.

Given the harmonic-arithmetic inequality $1/\langle 1/z \rangle \leq \langle z \rangle$, it is clear that, in the subsonic regime, the macroscopic mass density is always positive. However, the macroscopic stiffness becomes negative whenever

$$\frac{1}{\langle 1/z\rangle\langle z\rangle}c^2 \leq c_m^2 < c^2.$$

In this case, both macroscopic phase velocities become of the same sign so that a directional bandgap opens at arbitrarily low frequencies. When equality occurs, κ^e and one of the V vanish. Conversely, at supersonic speeds, macroscopic stiffness is positive but macroscopic mass density is negative if

$$c^2 < c_m^2 \le \langle 1/z \rangle \langle z \rangle c^2$$
.

Here also, both values of V are of the same sign. Finally, at equality, one V is infinite and the macroscopic mass density is null.

When normalized by their values in the limit $c_m \to 0$, the above macroscopic parameters turn out to be dependent on two variables: the normalized modulation speed c_m/c and a non-dimensional impedance-contrast parameter $\langle z \rangle \langle 1/z \rangle$. The latter is always larger than 1 with equality occurring for a homogeneous medium. The normalized profiles are plotted in Fig. 5. Most remarkably, the profile of V is asymmetric (with respect to the horizontal axis) meaning that right-going and left-going waves have different phase velocities. Furthermore, in the region where either κ^e or ρ^e is negative, both branches of V have the same sign indicating the opening of a directional bandgap at arbitrarily low frequencies (see Fig. 6).

³ The velocity V_f is deduced from a purely kinematic consideration: if x(t) is the position of the wave front, then $\dot{x}(t) = c(x(t) - c_m t)$.

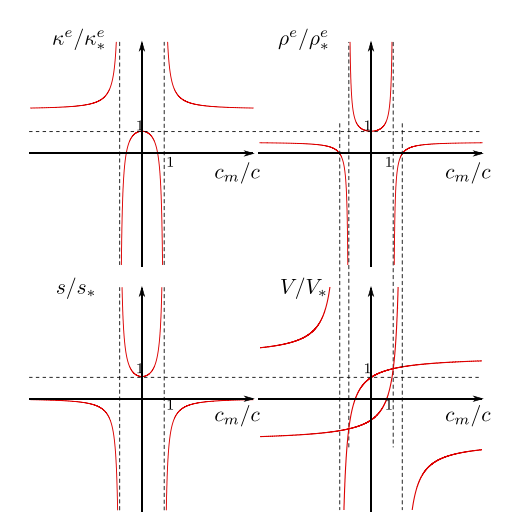


Fig. 5. The profiles of the normalized macroscopic constitutive parameters κ^e , ρ^e and s and of the macroscopic phase/group velocity V as functions of the modulation speed c_m . The normalization starred factors correspond to the values calculated for slow modulations (Section 2.6.1). At the excluded sonic modulation speed $c_m = c$, the macroscopic constitutive parameters diverge and the macroscopic group velocities become the same. Group velocities diverge when the macroscopic mass density is zero. For these plots, the contrast is such that $\langle z \rangle \langle 1/z \rangle = 2$.

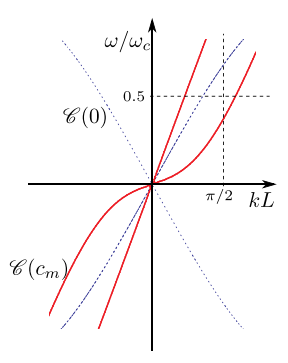


Fig. 6. The low-frequency part of the dispersion curve of a 1D laminate: with $(\mathscr{C}(c_m)$, in red solid lines) and without $(\mathscr{C}(0)$, in blue dotted lines) modulation. The corresponding laminate has two phases with medium contrasts of $\kappa_1/\kappa_2 = \rho_1/\rho_2 = 9$ ($\langle z \rangle \langle 1/z \rangle \approx 2$). The modulation speed c_m is 2c/3. At this value, κ^e is negative so that both macroscopic phase velocities have the same sign and a directional bandgap exists at arbitrarily low frequencies. (For interpretation of the references to colour in this figure legend, the reader is referred to the web version of this article.)

2.7. Numerical simulations of transient responses

To validate our theoretical findings, the transient response of a finite slab of a modulated phononic crystal is numerically simulated using the finite element method implemented by the commercial code COMSOL Multiphysics. The considered phononic crystal has two phases of equal thickness L/2=1 cm. The constitutive properties of the first phase are $\kappa_1=7$ GPa and $\rho_1=2800\,\mathrm{kg/m^3}$ whereas those of the second phase are given by $\kappa_2=\kappa_1/20$ and $\rho_2=\rho_1/20$ so that $c_1=c_2$. The slab has a total thickness of 280L and is loaded longitudinally at its centre point with a transient narrow-band excitation F(t). The behaviour of the non-modulated phononic crystal is systematically compared to that of the one rapidly modulated at the subsonic speed $c_m=0.2c_1=0.2c_2=1000\,\mathrm{m/s}$.

To track the wave propagation in the system, the transient wave fields at discrete locations are presented in Fig. 7. For comparison, the transient wave fields for the non-modulated phononic crystal are also included. The transient responses were simulated for two loadings. The first one (see Fig. 7(a)) has a central frequency $f_1 \approx 25$, 4 kHz falling within a directional bandgap of the modulated medium and within a total passing band of the non-modulated medium. The radiated wave is expected thus to propagate to the right exclusively in the presence of the modulation and in both directions in its absence (see Fig. 7(b, c)). The second loading (see Fig. 7(c)) has a central frequency $f_2 \approx 12$, 7 kHz which is in the first total passing band of both the modulated and non-modulated media. Emitted waves propagate to the left and to the right. Nonetheless, in the modulated medium, the modulation introduces a well-pronounced bias breaking time-reversal symmetry so that right-going and left-going waves have manifestly different velocities (Fig. 7(e, f)).

The dispersion diagram is obtained numerically by computing the space-time Fourier transform of the transient response of the phononic crystal under a broad-band excitation F(t) with a central frequency $f_3 \approx 63$, 6 kHz. The excitation force F(t)

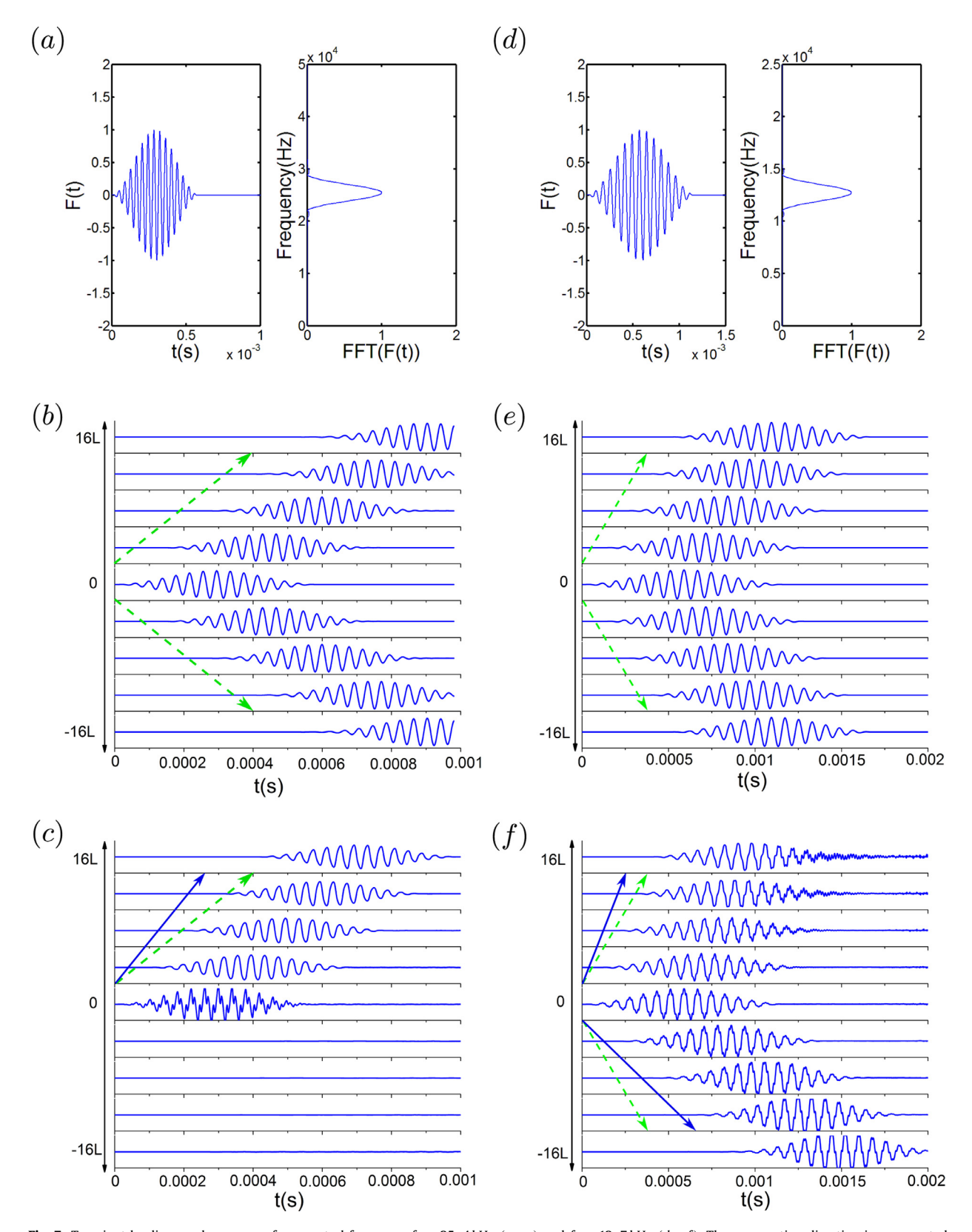


Fig. 7. Transient loadings and responses for a central frequency $f_1 \approx 25$, 4 kHz (a-c) and $f_2 \approx 12$, 7 kHz (d-f). The propagation direction is represented, for $c_m = 0$, by dashed green arrows and, for $c_m \neq 0$, by solid blue ones. For $c_m = 0$, wave propagation is symmetric (b, e). For $c_m \neq 0$, right-going waves are accelerated (c, f) and left-going waves are blocked at f_1 (c) and decelerated at f_2 (f). (For interpretation of the references to colour in this figure legend, the reader is referred to the web version of this article.)

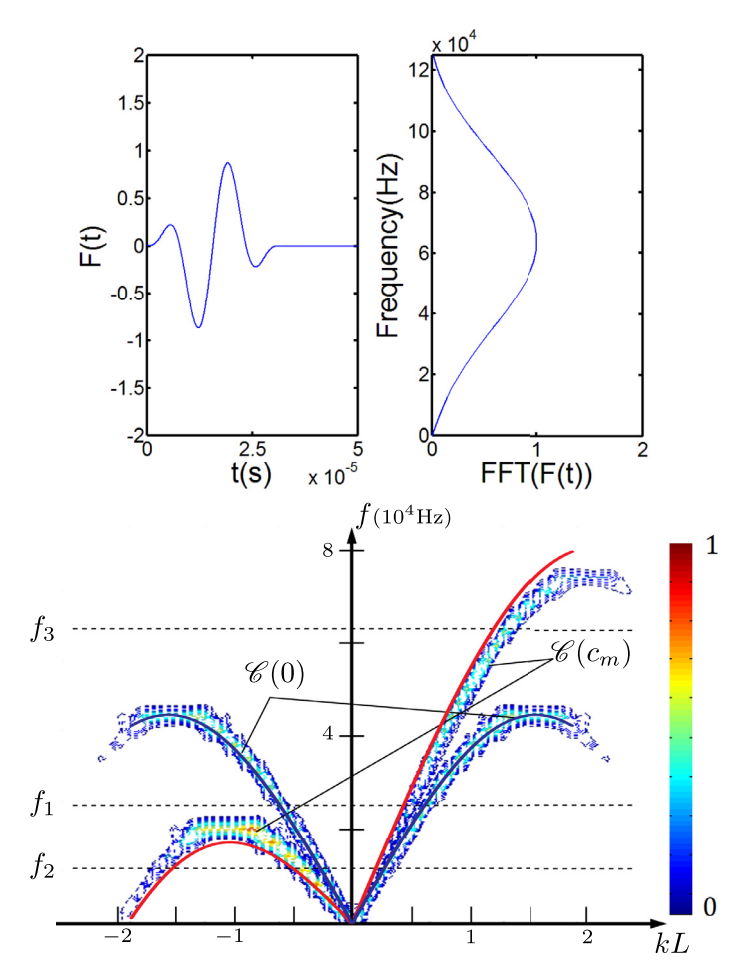


Fig. 8. The transient body force loading F in time (top left) and frequency (top right) domains. The corresponding transient response is analysed and its components plotted as level sets in the $(k, f = 2\pi\omega)$ -domain to generate the dispersion diagram (bottom). The components amplitudes are normalized to have values between 0 and 1 on an arbitrary scale (color bar). Solid lines correspond to the dispersion diagram of Eq. (11). (For interpretation of the references to colour in this figure legend, the reader is referred to the web version of this article.)

as well as its modal density distribution and the generated dispersion diagram are plotted in Fig. 8. Note that in order to facilitate the convergence of the numerical method, the Heaviside function describing the two-phase geometry was smoothed. As a consequence, the computed dispersion diagram differs slightly from the one obtained analytically through Eq. (11).

3. Wave propagation in 3D modulated laminates

Next, the constitutive behaviour of a laminate modulated at a finite speed c_m is derived in a full anisotropic elasticity 3D context. This behaviour is valid in the rigorous homogenization limit and is shown to be of the Willis type. Closed form analytical expressions of the various macroscopic constitutive parameters, including the Willis coupling tensors, are given in terms of the phases constitutive parameters and of the modulation speed.

3.1. Governing equations

Consider a periodic elastic laminate in d, say 3, dimensions (Fig. 9). Its stiffness tensor C and mass density ρ are periodic functions of one space coordinate, hereafter called x, carried by a unit vector denoted $\mathbf{n} (= \nabla x)$ and are independent of the other d-1 spatial coordinates. When time-modulated at speed c_m , C and ρ become periodic functions of $x-c_mt$:

$$\mathbf{C}(\mathbf{x},t) = \mathbf{C}(\mathbf{x} - c_m t), \quad \rho(\mathbf{x},t) = \rho(\mathbf{x} - c_m t).$$

Note that a modulation at speed c_m in a direction other than n is equivalent to a modulation at speed $c_m \cdot n$ in the direction of n due to the layered geometry.

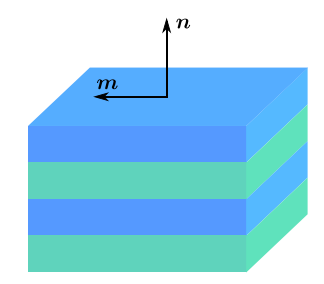


Fig. 9. A sketch of a 3D two-phase laminate, Direction n is the lamination direction whereas m is a generic orthogonal direction.

These constitutive parameters relate the stress tensor σ to the infinitesimal strain tensor e and the momentum field p to the velocity field v, according to

$$\sigma = \mathbf{C} : \boldsymbol{\varepsilon}, \quad \mathbf{p} = \rho \mathbf{v}.$$

The equilibrium of momentum dictates that

$$\nabla \cdot \boldsymbol{\sigma} = \partial_t \boldsymbol{p}$$
.

Last, strain and velocity derive from the same displacement field \boldsymbol{u}

$$\boldsymbol{\varepsilon} = \boldsymbol{\nabla} \otimes^{s} \boldsymbol{u}, \quad \boldsymbol{v} = \partial_{t} \boldsymbol{u}.$$

Therefore, the equation of motion written in terms of \boldsymbol{u} with full dependencies is

$$\nabla \cdot [\mathbf{C}(x - c_m t) : (\nabla \otimes^{\mathbf{s}} \mathbf{u}(\mathbf{x}, t))] = \partial_t (\rho(x - c_m t) \partial_t \mathbf{u}(\mathbf{x}, t)).$$

3.2. Two-scale asymptotic expansions

Adapting standard two-scale asymptotic homogenization procedure (see, e.g., Sanchez-Palencia, 1980), we look for displacement solutions in the form

$$\mathbf{u} = \mathbf{u}(\mathbf{x}, \mathbf{x} - c_m t, t)$$

where $\mathbf{u}(\mathbf{x}, \xi, t)$ is a solution to the motion equation

$$(\nabla + \mathbf{n}\partial_{\xi}) \cdot \{ \mathbf{C}(\xi) : [(\nabla + \mathbf{n}\partial_{\xi}) \otimes^{s} \mathbf{u}(\mathbf{x}, \xi, t)] \} = (\partial_{t} - c_{m}\partial_{\xi}) [\rho(\xi)(\partial_{t} - c_{m}\partial_{\xi}) \mathbf{u}(\mathbf{x}, \xi, t)]$$

and is an L-periodic function of ξ where L is the unit cell thickness in the direction n.

In the homogenization limit, L is infinitely small compared to the wavelength of travelling waves and ξ describes a mixed space-time fast variable whereas \mathbf{x} and t describe slow variables. Thus, derivatives with respect to ξ yield larger variations than derivatives with respect to both \mathbf{x} and t. The equation of motion is scaled accordingly into

$$\left(\nabla + \mathbf{n}\frac{\partial_{\xi}}{\epsilon}\right) \cdot \left\{\mathbf{C}(\xi) : \left[\left(\nabla + \mathbf{n}\frac{\partial_{\xi}}{\epsilon}\right) \otimes^{s} \mathbf{u}^{\epsilon}(\mathbf{x}, \xi, t)\right]\right\} = \left(\partial_{t} - c_{m}\frac{\partial_{\xi}}{\epsilon}\right) \left[\rho(\xi)\left(\partial_{t} - c_{m}\frac{\partial_{\xi}}{\epsilon}\right) \mathbf{u}^{\epsilon}(\mathbf{x}, \xi, t)\right]$$
(16)

where the limit $\epsilon \to 0$ now corresponds to the homogenization limit.

Finally, the scaled displacement field is expanded into the asymptotic series

$$u^{\epsilon}(\mathbf{x}, \xi, t) = \mathbf{U}(\mathbf{x}, \xi, t) + \epsilon \delta \mathbf{u}(\mathbf{x}, \xi, t) + O(\epsilon^{2}). \tag{17}$$

U being the macroscopic displacement we wish to characterize and δu being its first order correction.

3.3. Scale separation

Inserting the expansion (17) into the scaled motion Eq. (16) and keeping the lowest order terms, those proportional to ϵ^{-2} , yields

$$\mathbf{n}\partial_{\xi}\cdot\left[\mathbf{C}(\xi):\left(\mathbf{n}\partial_{\xi}\otimes^{s}\mathbf{U}(\mathbf{x},\xi,t)\right)\right]=c_{m}^{2}\partial_{\xi}\left(\rho(\xi)\partial_{\xi}\mathbf{U}(\mathbf{x},\xi,t)\right).$$

When contracted with U and integrated with respect to ξ over a unit cell, the above equation yields

$$\int_{0}^{L} \partial_{\xi} \boldsymbol{U}(\boldsymbol{x}, \xi, t) \cdot (\boldsymbol{n} \cdot \boldsymbol{C}(\xi) \cdot \boldsymbol{n} - c_{m}^{2} \rho(\xi) \boldsymbol{I}) \cdot \partial_{\xi} \boldsymbol{U}(\boldsymbol{x}, \xi, t) \, \mathrm{d}\xi = 0, \tag{18}$$

where I is the second order identity tensor.

Now, we make the assumption that

$$\mathbf{n} \cdot \mathbf{C}(\xi) \cdot \mathbf{n} - c_m^2 \rho(\xi) \mathbf{I}$$

is definite positive for all ξ or definite negative for all ξ . This means that c_m does not exceed any of the phase velocities in direction \boldsymbol{n} or exceeds all of them at once; a guarantee of continuity, as mentioned earlier. Note that \boldsymbol{C} is possibly anisotropic and that c_m is allowed to match phase velocity in directions other than \boldsymbol{n} .

These considerations allow us to conclude that the integrand in (18) has a constant sign, implying

$$\partial_{\varepsilon} \mathbf{U} = \mathbf{0}$$
.

Thus, to the leading order, the displacement U does not depend on the fast variable ξ . The macroscopic and microscopic scales described respectively by (x, t) and ξ are therefore separated.

3.4. Localization tensors

The second step, after scale separation, is to derive localization tensors which yield the microscopic variations of δu in terms of the macroscopic strain and velocity fields.

Inserting again (17) into (16) and keeping the terms proportional to ϵ^{-1} results in

$$\mathbf{n}\partial_{\xi}\cdot\left[\mathbf{C}:\left(\mathbf{n}\partial_{\xi}\otimes^{s}\delta\mathbf{u}+\mathbf{E}\right)\right]=-c_{m}\partial_{\xi}\left[\rho\left(-c_{m}\partial_{\xi}\delta\mathbf{u}+\mathbf{V}\right)\right],\tag{19}$$

where explicit dependencies have been dropped to improve readability and

$$\mathbf{E} = \mathbf{E}(\mathbf{x}, t) = \nabla \otimes^{\mathrm{s}} \mathbf{U}(\mathbf{x}, t), \quad \mathbf{V} = \mathbf{V}(\mathbf{x}, t) = \partial_t \mathbf{U}(\mathbf{x}, t),$$

are the macroscopic strain and velocity fields, respectively.

The foregoing motion equation is a linear second order ordinary differential equation which can be integrated once into

$$(\mathbf{n} \cdot \mathbf{C} \cdot \mathbf{n} - c_m^2 \rho \mathbf{I}) \cdot \partial_{\varepsilon} \delta \mathbf{u} = \boldsymbol{\alpha} - \mathbf{n} \cdot \mathbf{C} : \mathbf{E} - c_m \rho \mathbf{V}$$

with α being an integration constant, or rather ξ -independent, vector. The inequality constraint imposed upon c_m means that the second order tensor

$$\Gamma = (\mathbf{n} \cdot \mathbf{C} \cdot \mathbf{n} - c_m^2 \rho \mathbf{I})^{-1} \tag{20}$$

is well defined, symmetric and either positive or negative definite. Thus, we have

$$\partial_{\varepsilon} \delta \mathbf{u} = \mathbf{\Gamma} \cdot (\boldsymbol{\alpha} - \mathbf{n} \cdot \mathbf{C} : \mathbf{E} - c_m \rho \mathbf{V}).$$

When averaged with respect to ξ , the left hand side above vanishes by periodicity and we are left with an equation which can be solved for α , namely,

$$\mathbf{0} = \langle \mathbf{\Gamma} \rangle \cdot \boldsymbol{\alpha} - \langle \mathbf{\Gamma} \otimes \boldsymbol{n} : \boldsymbol{C} \rangle : \boldsymbol{E} - c_m \langle \rho \mathbf{\Gamma} \rangle \cdot \boldsymbol{V}.$$

Therefore.

$$\alpha = \langle \Gamma \rangle^{-1} \cdot \langle \Gamma \otimes \mathbf{n} : \mathbf{C} \rangle : \mathbf{E} + c_m \langle \Gamma \rangle^{-1} \cdot \langle \rho \Gamma \rangle \cdot \mathbf{V}$$

since an average of positive or negative definite tensors, such as $\langle \Gamma \rangle$, is again positive or negative definite, ergo invertible. Concluding, the localization equation can be expressed as

$$\partial_{\varepsilon} \delta \mathbf{u} = \mathbf{\Gamma} \cdot \left(\langle \mathbf{\Gamma} \rangle^{-1} \cdot \langle \mathbf{\Gamma} \otimes \mathbf{n} : \mathbf{C} \rangle - \mathbf{n} \cdot \mathbf{C} \right) : \mathbf{E} + c_{m} \mathbf{\Gamma} \cdot \left(\langle \mathbf{\Gamma} \rangle^{-1} \cdot \langle \rho \mathbf{\Gamma} \rangle - \rho \mathbf{I} \right) \cdot \mathbf{V}. \tag{21}$$

3.5. Macroscopic motion and constitutive equations

The macroscopic motion equation is obtained by averaging the scaled motion Eq. (16) and keeping leading order terms those proportional to ϵ^0 ,

$$\nabla \cdot \mathbf{\Sigma} = \partial_t \mathbf{P}$$

where Σ and P are identified as the macroscopic stress and momentum fields. They are given by

$$\Sigma = \langle C : (n\partial_{\xi} \otimes^{s} \delta u + E) \rangle, \quad P = \langle \rho(-c_{m}\partial_{\xi} \delta u + V) \rangle.$$

The macroscopic constitutive law follows from these by using the localization Eq. (21) of the previous paragraph. It takes the form

$$\Sigma = \mathbf{C}^e : \mathbf{E} + \mathbf{S}^1 \cdot \mathbf{V},$$

$$\mathbf{P} = \mathbf{S}^2 : \mathbf{E} + \boldsymbol{\rho}^e \cdot \mathbf{V},$$
(22)

where the fourth order effective stiffness tensor C^e , the third order Willis coupling tensors S^1 and S^2 , and the second order effective mass density tensor ρ^e have the analytical closed form expressions

$$C^{e} = \langle C \rangle + \langle C : n \otimes \Gamma \rangle \cdot \langle \Gamma \rangle^{-1} \cdot \langle \Gamma \otimes n : C \rangle - \langle C : n \otimes \Gamma \otimes n : C \rangle,$$

$$S^{1} = c_{m} \langle C : n \otimes \Gamma \rangle \cdot \langle \Gamma \rangle^{-1} \cdot \langle \rho \Gamma \rangle - c_{m} \langle \rho C : n \otimes \Gamma \rangle,$$

$$\mathbf{S}^{2} = -c_{m} \langle \rho \mathbf{\Gamma} \rangle \cdot \langle \mathbf{\Gamma} \rangle^{-1} \cdot \langle \mathbf{\Gamma} \otimes \mathbf{n} : \mathbf{C} \rangle + c_{m} \langle \rho \mathbf{\Gamma} \otimes \mathbf{n} : \mathbf{C} \rangle,$$

$$\boldsymbol{\rho}^{e} = \langle \rho \rangle \mathbf{I} - c_{m}^{2} \langle \rho \mathbf{\Gamma} \rangle \cdot \langle \mathbf{\Gamma} \rangle^{-1} \cdot \langle \rho \mathbf{\Gamma} \rangle + c_{m}^{2} \langle \rho^{2} \mathbf{\Gamma} \rangle.$$
(23)

The macroscopic constitutive law (22) couples stress to velocity and momentum to strain and is therefore of Willis form (Willis, 1997). There are however a number of properties that distinguish the present constitutive relation from the ones usually derived according to the Willis homogenization theory.

- 1. The present macroscopic constitutive law is derived and is valid in the rigorous homogenization limit where there is a clear scale separation as was demonstrated earlier.
- 2. The macroscopic constitutive parameters are all local in both space and time and, as such, are independent of the frequency and the wavenumber of the propagating waves.
- 3. These parameters are unique,
- 4. and real valued.

Most notably, the coupling tensors do not vanish in general at infinitely low frequencies.

On the other hand, due to the symmetry of C, Γ and ρI , the present macroscopic constitutive parameters satisfy the same symmetry properties as the Willis parameters:

$$\mathbf{C}^e = (\mathbf{C}^e)^T, \quad \boldsymbol{\rho}^e = (\boldsymbol{\rho}^e)^T, \quad \mathbf{S}^1 = -(\mathbf{S}^2)^T. \tag{24}$$

Using index notation, these become $C^e_{ijkl} = C^e_{klij}$, $\rho^e_{ij} = \rho^e_{ji}$ and $S^1_{ijk} = -S^2_{ijk}$. In addition, the symmetry of stress and strain imposes the constraints $C^e_{ijkl} = C^e_{jikl}$ and $S^1_{ijk} = S^1_{jik}$. All of these properties follow from the analytical expressions (23).

Note that the Willis coupling vanishes when either ρ or \mathbf{C} is uniform. Conversely, the existence of a non-vanishing Willis coupling requires that both \mathbf{C} and ρ are modulated. The effective density remains unchanged with $\rho^e = \rho \mathbf{I}$ if ρ is uniform; hence, anisotropic density requires modulation of the density. The standard macroscopic constitutive behaviour of a laminate is recovered in the absence of time modulations, i.e., for $c_m = 0$ we obtain the spatially averaged homogenization result. In the opposite extreme of infinite modulation speeds, $c_m \to \infty$, the calculated macroscopic behaviour is exact rather than asymptotic and the macroscopic constitutive parameters simplify to the alternative averages

$$\mathbf{C}^e = \langle \mathbf{C} \rangle, \quad \mathbf{S}^1 = \mathbf{S}^2 = \mathbf{0}, \quad \boldsymbol{\rho}^e = \langle \rho^{-1} \rangle^{-1} \mathbf{I}.$$

3.6. Example: slow modulation of isotropic layers

A 1D example was thoroughly investigated in Section 2. In higher dimensions d > 1, it is of interest to see how the formulae (23) can be applied for, say, a slowly modulated laminate. In this case, C^e is simply the macroscopic stiffness tensor of the non-modulated laminate and its calculation is extensively discussed in the literature. As for the macroscopic mass density, it reduces to the arithmetic mean of mass densities. Explicit expressions for the Willis coupling tensors S^1 and S^2 are derived next for the particular example of isotropic layers.

The elastic stiffness tensor of an isotropic medium is, using index notations,

$$C_{ijkl} = \mu(\delta_{ik}\delta_{il} + \delta_{il}\delta_{ik}) + \lambda\delta_{ij}\delta_{kl},$$

where δ is the Kronecker delta and (μ, λ) the Lamé coefficients. The acoustic tensor in direction \boldsymbol{n} is therefore

$$\mathbf{n} \cdot \mathbf{C} \cdot \mathbf{n} = (\mu + \lambda)\mathbf{n} \otimes \mathbf{n} + \mu \mathbf{I}$$
.

Let m span the directions orthogonal to n in an orthonormal basis of the d-dimensional space, such that $I = n \otimes n + m \otimes m$ with m summed over d-1 dimensions. Then,

$$\mathbf{n} \cdot \mathbf{C} \cdot \mathbf{n} = (2\mu + \lambda)\mathbf{n} \otimes \mathbf{n} + \mu \mathbf{m} \otimes \mathbf{m}$$
.

Since c_m^2 is neglected, the inverse of this expression yields the explicit result

$$\Gamma = \frac{1}{2\mu + \lambda} \mathbf{n} \otimes \mathbf{n} + \frac{1}{\mu} \mathbf{m} \otimes \mathbf{m}.$$

The preliminary calculations

$$\mathbf{n} \otimes \mathbf{\Gamma} = \frac{1}{2\mu + \lambda} \mathbf{n} \otimes \mathbf{n} \otimes \mathbf{n} + \frac{1}{\mu} \mathbf{n} \otimes \mathbf{m} \otimes \mathbf{m},$$

$$\mathbf{C}: (\mathbf{a} \otimes \mathbf{b}) = 2\mu \mathbf{a} \otimes^{s} \mathbf{b} + \lambda (\mathbf{a} \cdot \mathbf{b}) \mathbf{I}$$

together yield

$$\mathbf{C}: \mathbf{n} \otimes \mathbf{\Gamma} = \frac{1}{2\mu + \lambda} (2\mu \mathbf{n} \otimes \mathbf{n} + \lambda \mathbf{I}) \otimes \mathbf{n} + \frac{1}{\mu} (2\mu \mathbf{n} \otimes^{s} \mathbf{m}) \otimes \mathbf{m}$$
$$= \mathbf{n} \otimes \mathbf{n} \otimes \mathbf{n} + \frac{\lambda}{2\mu + \lambda} \mathbf{m} \otimes \mathbf{m} \otimes \mathbf{n} + 2\mathbf{n} \otimes^{s} \mathbf{m} \otimes \mathbf{m}.$$

Upon calculating in the same manner the remaining terms in the expression of S^1 , it can be concluded that

$$\begin{split} \mathbf{S}^{1}/c_{m} &= \left(\frac{\langle \rho/(2\mu+\lambda)\rangle}{\langle 1/(2\mu+\lambda)\rangle} - \langle \rho \rangle\right) \mathbf{n} \otimes \mathbf{n} \otimes \mathbf{n} + \left(\frac{\langle \lambda/(2\mu+\lambda)\rangle\langle \rho/(2\mu+\lambda)\rangle}{\langle 1/(2\mu+\lambda)\rangle} - \langle \rho \lambda/(2\mu+\lambda)\rangle\right) \mathbf{m} \otimes \mathbf{m} \otimes \mathbf{n} \\ &+ 2 \left(\frac{\langle \rho/\mu\rangle}{\langle 1/\mu\rangle} - \langle \rho \rangle\right) \mathbf{n} \otimes^{s} \mathbf{m} \otimes \mathbf{m}. \end{split}$$

A macroscopic velocity oriented in the direction of the modulation \boldsymbol{n} therefore generates normal stresses in all directions \boldsymbol{n} and \boldsymbol{m} whereas a macroscopic velocity normal to the direction of modulation will generate shear stresses in all the planes (\boldsymbol{n} , \boldsymbol{m}). Each time, the generated stresses are proportional to the calculated coupling parameters which in turn are proportional to some contrast measure and to the modulation speed c_m .

3.7. Macroscopic dispersion relation

In terms of the macroscopic displacement field, the macroscopic motion equation is

$$\nabla \cdot [\mathbf{C}^e : (\nabla \otimes^s \mathbf{U}) + \mathbf{S}^1 \cdot \partial_t \mathbf{U}] = \partial_t [\mathbf{S}^2 : (\nabla \otimes^s \mathbf{U}) + \boldsymbol{\rho}^e \cdot \partial_t \mathbf{U}].$$

For a plane wave of wavenumber k and frequency ω , the amplitude U is a solution to the eigenvalue problem

$$(\mathbf{k} \cdot \mathbf{C}^e \cdot \mathbf{k} - 2\omega \mathbf{k} \cdot \mathbf{S} - \omega^2 \rho^e) \cdot \mathbf{U} = \mathbf{0}.$$

We have combined the coupling tensors S^1 and S^2 into one tensor with components

$$S_{ijk} = \frac{1}{2} \left(S_{ijk}^1 - S_{jik}^2 \right) = \frac{1}{2} \left(S_{ijk}^1 + S_{ikj}^1 \right) \tag{25}$$

implying $\mathbf{k} \cdot \mathbf{S} = (\mathbf{k} \cdot \mathbf{S})^T$. The macroscopic dispersion relation follows as

$$\det(\mathbf{k}\cdot\mathbf{C}^e\cdot\mathbf{k}-2\omega\mathbf{k}\cdot\mathbf{S}-\omega^2\boldsymbol{\rho}^e)=0.$$

Thus, non-reciprocity caused by time modulations on the microscale is generally enforced on the macroscale by the Willis coupling tensor *S*.

The 1D examples treated in the first section show that the macroscopic dispersion equation does admit solutions. In the general case however, the existence of propagating macroscopic modes at arbitrarily low non-null frequencies is not obvious at all from the above macroscopic dispersion relation. The bounds we obtain in the next section will help prove that a modulated periodic laminate in fact does allow low-frequency wave propagation.

4. Energy considerations

Even though formulae (23) are sufficient for calculation purposes, some general properties satisfied by the macroscopic constitutive parameters are better understood from simple approximations or bounds derived next. An adapted version of the Hill–Mandel relation (Zaoui, 2002) will provide a first bound. A second bound stems from convexity/concavity of the potential energy. Positive-definiteness, or lack thereof, of the macroscopic stiffness tensor and of the macroscopic mass density as well as the existence of real macroscopic phase velocities are discussed and the conservation of energy is considered.

4.1. Hill-Mandel relation: a first elementary bound

The microscopic states of strain and velocity, to leading order, follow from Eq. (19) as

$$\boldsymbol{\varepsilon} = \boldsymbol{n} \partial_{\varepsilon} \otimes^{s} \delta \boldsymbol{u} + \boldsymbol{E}, \quad \boldsymbol{v} = -c_{m} \partial_{\varepsilon} \delta \boldsymbol{u} + \boldsymbol{V},$$

whereas the corresponding states of stress and momentum are called $\sigma (= C \varepsilon)$ and $p (= \rho v)$ as before. Let $(\delta u, E, V)$ and $(\delta u', E', V')$ be two sets of solutions, with similar notations for ε' , v', σ' and p'. A direct application of the virtual work theorem to Eq. (19) yields

$$\langle (\mathbf{n}\partial_{\varepsilon}\otimes^{s}\delta\mathbf{u}'):\boldsymbol{\sigma}\rangle = \langle -c_{m}\partial_{\varepsilon}\delta\mathbf{u}'\cdot\boldsymbol{p}\rangle,$$

or,

$$\langle (\boldsymbol{\varepsilon}' - \boldsymbol{E}') : \boldsymbol{\sigma} \rangle = \langle (\boldsymbol{v}' - \boldsymbol{V}') \cdot \boldsymbol{p} \rangle.$$

In conclusion, the Hill-Mandel relation stating the equality between the microscopic and macroscopic virtual works,⁴ to leading order, holds in the form

$$\langle \boldsymbol{\varepsilon}' : \boldsymbol{\sigma} - \boldsymbol{v}' \cdot \boldsymbol{p} \rangle = \langle \boldsymbol{\varepsilon}' \rangle : \langle \boldsymbol{\sigma} \rangle - \langle \boldsymbol{v}' \rangle \cdot \langle \boldsymbol{p} \rangle = \boldsymbol{E}' : \boldsymbol{\Sigma} - \boldsymbol{V}' \cdot \boldsymbol{P}$$

where the final identity follows from the definitions $\mathbf{E} = \langle \boldsymbol{\varepsilon} \rangle$, etc.

⁴ Or Lagrangian densities more accurately.

Incidentally, note that the symmetry of the left-most term, namely ε' : $\sigma = \varepsilon'$: σ' and $\upsilon' \cdot p = \upsilon \cdot p'$, induces a similar symmetry on the right-most term. It follows immediately that

$$\mathbf{E}': \mathbf{\Sigma} - \mathbf{V}' \cdot \mathbf{P} = \mathbf{E}: \mathbf{\Sigma}' - \mathbf{V} \cdot \mathbf{P}'. \tag{26}$$

This provides a second proof of the symmetry properties of the macroscopic constitutive law in Eq. (24).

In order to obtain a first elementary bound, let $\mathbf{V}' = \mathbf{V}$ and

$$\boldsymbol{E}' = \boldsymbol{E} = -\frac{1}{C_m} \boldsymbol{n} \otimes^{\mathrm{s}} \boldsymbol{V}.$$

Expanding the various terms in the Hill-Mandel relation (26) and factoring leads to

$$\langle (-c_m \partial_{\varepsilon} \delta \mathbf{u} + \mathbf{V}) \cdot \mathbf{\Gamma}^{-1} \cdot (-c_m \partial_{\varepsilon} \delta \mathbf{u} + \mathbf{V}) \rangle = \mathbf{V} \cdot (\mathbf{n} \cdot \mathbf{C}^e \cdot \mathbf{n} - 2c_m \mathbf{n} \cdot \mathbf{S} - c_m^2 \boldsymbol{\rho}^e) \cdot \mathbf{V}.$$

This expression therefore has the same sign as Γ and is positive definite in the subsonic regime and negative definite in the supersonic regime. Accordingly, a first elementary bound on the macroscopic constitutive parameters is

$$\mathbf{n} \cdot \mathbf{C}^e \cdot \mathbf{n} - 2c_m \mathbf{n} \cdot \mathbf{S} - c_m^2 \boldsymbol{\rho}^e > (<)0.$$

Above and below, when inequalities are written with two signs, it means that the first sign applies in the subsonic regime whereas the second, parenthesised, applies in the supersonic regime.

4.2. A second elementary bound

The quadratic form $\mathbf{n} \cdot \mathbf{C} \cdot \mathbf{n} - c_m^2 \rho \mathbf{I} (= \mathbf{\Gamma}^{-1})$ defines a strictly convex (resp. concave) potential in the subsonic (resp. supersonic) regime. Therefore, the solution $\delta \mathbf{u}$ to Eq. (19) minimizes (resp. maximizes) the energy functional

$$\left\langle \frac{1}{2} \partial_{\xi} \delta \mathbf{u}' \cdot \mathbf{\Gamma}^{-1} \cdot \partial_{\xi} \delta \mathbf{u}' + (\mathbf{n} \partial_{\xi} \otimes^{s} \delta \mathbf{u}') : \mathbf{C} : \mathbf{E} + c_{m} \partial_{\xi} \delta \mathbf{u}' \cdot (\rho \mathbf{V}) \right\rangle$$

among all periodic continuous fields $\delta u'$. Taking $\delta u' = 0$ in particular yields

$$\left\langle \frac{1}{2} \partial_{\xi} \delta \mathbf{u} \cdot \mathbf{\Gamma}^{-1} \cdot \partial_{\xi} \delta \mathbf{u} + (\mathbf{n} \partial_{\xi} \otimes^{s} \delta \mathbf{u}) : \mathbf{C} : \mathbf{E} + c_{m} \partial_{\xi} \delta \mathbf{u} \cdot (\rho \mathbf{V}) \right\rangle \leq (\geq) 0.$$

Then, with the help of the virtual work theorem,

$$\langle (\mathbf{n}\partial_{\xi}\otimes^{s}\delta\mathbf{u}): \mathbf{C}: \mathbf{E}+c_{m}\partial_{\xi}\delta\mathbf{u}\cdot(\rho\mathbf{V})\rangle\leq (\geq)0,$$

or

$$\langle (\boldsymbol{\sigma} - \boldsymbol{C} : \boldsymbol{E}) : \boldsymbol{E} - (\boldsymbol{p} - \rho \boldsymbol{V}) \cdot \boldsymbol{V} \rangle \leq (\geq) 0.$$

Finally,

$$\Sigma : E - P \cdot V \leq (\geq)E : \langle C \rangle : E - \langle \rho \rangle V \cdot V$$
.

Written in terms of constitutive laws, the second elementary bound is

$$\begin{bmatrix} \mathbf{C}^e & \mathbf{S}^1 \\ -\mathbf{S}^2 & -\boldsymbol{\rho}^e \end{bmatrix} \leq (\geq) \begin{bmatrix} \langle \mathbf{C} \rangle & \mathbf{0} \\ \mathbf{0} & -\langle \rho \rangle \mathbf{I} \end{bmatrix}.$$

This bound guarantees positive-definiteness for the macroscopic mass density tensor in the subsonic regime and for the macroscopic stiffness tensor in the supersonic regime. Conversely, the macroscopic stiffness can become singular or even negative in the subsonic regime. The same conclusion holds for the macroscopic density in the supersonic regime. Examples were given in Section 2.6.

4.3. Repercussions on the macroscopic dispersion curve

In non-modulated media, the existence of low-frequency macroscopic waves is a consequence to the positivity of the macroscopic elastic stiffness tensor and of mass density. In resonant metamaterials for instance, it is known that a negative stiffness or a negative mass density introduces a bandgap in the dispersion curve. In contrast, for the modulated laminate, we prove in this subsection that no total bandgaps appear even when the macroscopic stiffness or mass density becomes negative.

More specifically, let U be a macroscopic plane wave of frequency ω and wavenumber k propagating in the modulation direction \boldsymbol{n} . The phase velocity $V = \omega/k$ is therefore a solution to the dispersion equation

$$\det \Lambda(V) = 0$$
,

where $\Lambda(V)$ is the second order tensor

$$\mathbf{\Lambda}(V) = \mathbf{n} \cdot \mathbf{C}^e \cdot \mathbf{n} - 2V\mathbf{n} \cdot \mathbf{S} - V^2 \boldsymbol{\rho}^e.$$

Our purpose is to prove that this equation has real solutions. The argument below is presented for subsonic modulations. A similar argument is available for supersonic modulations but is skipped.

In the subsonic regime, ρ^e is a positive definite tensor as it is larger than $\langle \rho \rangle I$ by the second elementary bound. Thus, when V approaches $\pm \infty$, $\Lambda(V)$ becomes asymptotic to $-V^2\rho^e$ and has only negative eigenvalues. On the other hand, we know that $\Lambda(c_m)$ is a positive definite tensor thanks to the first elementary bound. Consequently, when V goes from $-\infty$, to c_m , to $+\infty$, the eigenvalues of $\Lambda(V)$ go from negative, to positive then to negative again. Hence, by continuity, each eigenvalue of $\Lambda(V)$ vanishes twice and det $\Lambda(V)$ vanishes 2d times (counted with multiplicity). In conclusion, a modulated laminate has d acoustic branches. The phase velocity directions associated with these branches remain however undetermined and are in general unevenly distributed due to the breaking of time-reversal symmetry.

This existence result is how the inequality $s^2 + \rho^e c^e > 0$ seen in Section 2.6 generalizes to arbitrary dimensions.

4.4. A remark on energy conservation

The equation of conservation of energy reads

$$\partial_t \mathscr{E} - \nabla \cdot (\boldsymbol{v} \cdot \boldsymbol{\sigma}) = \frac{1}{2} \boldsymbol{\varepsilon} : \partial_t \boldsymbol{C} : \boldsymbol{\varepsilon} - \frac{1}{2} \partial_t \rho \boldsymbol{v} \cdot \boldsymbol{v},$$

where $\mathscr E$ is the total potential and kinetic energy, $-\boldsymbol{v}\cdot\boldsymbol{\sigma}$ is energy flux and the right-hand term is an energy source/sink due to the time modulation of the constitutive properties.

As for the macroscopic scale, a pseudo-energy density ${\mathscr F}$ similar to ${\mathscr E}$ can be defined through

$$\mathscr{F} = \frac{1}{2}\mathbf{\Sigma} : \mathbf{E} + \frac{1}{2}\mathbf{P} \cdot \mathbf{V}.$$

Then, the macroscopic motion equation along with the symmetries satisfied by the macroscopic constitutive parameters guarantee that the equation of conservation of pseudo-energy

$$\partial_t \mathscr{F} - \nabla \cdot (\mathbf{V} \cdot \mathbf{\Sigma}) = 0$$

holds. At first sight, it looks like the microscopic energy source/sink has no effects on the macroscopic scale. This is not true however. In fact, the macroscopic equation of conservation of energy is

$$\partial_t \langle \mathscr{E} \rangle - \nabla \cdot \langle \boldsymbol{v} \cdot \boldsymbol{\sigma} \rangle = \left\langle \frac{1}{2} \boldsymbol{\varepsilon} : \partial_t \boldsymbol{C} : \boldsymbol{\varepsilon} - \frac{1}{2} \partial_t \rho \boldsymbol{v} \cdot \boldsymbol{v} \right\rangle$$

and, in general,

$$\mathscr{F} \neq \langle \mathscr{E} \rangle, \quad \mathbf{V} \cdot \mathbf{\Sigma} \neq \langle \mathbf{v} \cdot \mathbf{\sigma} \rangle, \quad \left\langle \frac{1}{2} \boldsymbol{\varepsilon} : \partial_t \mathbf{C} : \boldsymbol{\varepsilon} - \frac{1}{2} \partial_t \rho \boldsymbol{v} \cdot \boldsymbol{v} \right\rangle \neq 0.$$

A side effect is that the macroscopic energy velocity obtained as the ratio of the macroscopic energy flux to the macroscopic energy density, i.e.,

$$-\frac{\langle \boldsymbol{v} \cdot \boldsymbol{\sigma} \rangle}{\langle \mathscr{E} \rangle}$$

is different from the macroscopic group velocity, previously denoted V, and equal to the ratio of the pseudo-energy flux to the pseudo-energy density

$$-rac{oldsymbol{V}\cdotoldsymbol{\Sigma}}{\mathscr{F}}$$

Indeed, the latter can become infinite whereas the former is necessarily finite as was discussed in Section 2.6.

5. Conclusion

A periodic wave-like modulation of the constitutive parameters of a medium is sometimes referred to as a "pump wave". A wave propagating with the modulating pump wave is scattered differently than when it is propagating against it. This bias is equivalent to the breaking of time reversal symmetry and reciprocity of wave propagation in the modulated medium. To first order, i.e., for low-amplitude slow modulations, non-reciprocity is only visible near the edges of the different Brillouin zones. In a modulated medium, Bragg reflection occurs at different frequencies for left-going and right-going waves. In other words, a wave that is totally reflected when incident from the right can be totally transmitted if incident from the left and vice versa. In terms of bandgaps, total bandgaps are "sheared" into directional bandgaps.

As modulation speed and amplitude increase, non-reciprocity becomes visible at lower frequencies. Most remarkably, when both elastic moduli and mass density are strongly modulated, non-reciprocity manifests in the homogenization limit so that left- and right-going waves have different group velocities. These predicted anomalous wave phenomena were also verified by numerical simulations. The corresponding macroscopic constitutive behaviour turns out to be of the Willis type where the Willis stress-velocity and momentum-strain coupling tensor directly quantifies non-reciprocity and the bias in group velocities. Closed form analytical expressions of the macroscopic constitutive stiffness, mass density and coupling

tensors are obtained for modulated laminates in arbitrary dimensions extending thus the standard results for periodic (non-modulated) laminates. Finally, some elementary energy bounds based on extensions of the Hill–Mandel relation and the potential energy principle allow us to gain further insight into the structure of the macroscopic Willis constitutive law.

To the best of the authors' knowledge, the studied modulated laminates provide the first example of a genuine Willis behaviour, i.e., with a substantial Willis coupling, valid in the strictly scale-separated homogenization limit. Furthermore, the existence of simple closed-form analytical expressions makes it possible to tackle inverse problems, say, for cloaking applications, whereby the Willis parameters are given and the microstructure and the modulation are solved for. On the other hand, the practical feasibility of these modulated media, where stiffness and mass density change in time, is yet to be demonstrated. To that end, techniques such as magnetic stimuli in magnetorheological elastomers, trains of shock waves in soft materials, the photo-elastic effect, programmable piezoelectric circuits or a combination thereof could be exploited.

Acknowledgement

This work is supported by the Air Force Office of Scientific Research under Grant No. AF 9550-15-1-0016 with Program Manager Dr. Byung-Lip (Les) Lee and the NSF EFRI under award No. 1641078.

References

Amirkhizi, A.V., Nemat-Nasser, S., 2008. Microstructurally-based homogenization of electromagnetic properties of periodic media. Comptes Rendus Mécanique 336, 24–33.

Casadei, F., Delpero, T., Bergamini, A., Ermanni, P., Ruzzene, M., 2012. Piezoelectric resonator arrays for tunable acoustic waveguides and metamaterials. J. Appl. Phys. 112, 064902.

Cassedy, E.S., Oliner, A.A., 1963. Dispersion relations in time-Space periodic media: part I-Stable interactions. Proc. IEEE 51, 1342-1359.

Cassedy, E.S., Oliner, A.A., 1963. Dispersion relations in time-Space periodic media: part II-Unstable interactions. Proc. IEEE 51, 1342-1359.

Chen, Y.Y., Hu, G.K., Huang, G.L., 2016. An adaptive metamaterial beam with hybrid shunting circuits for extremely broadband control of flexural waves. Smart Mater. Struct. 25, 105036.

Chen, Y.Y., Huang, G.L., Sun, C.T., 2014. Band gap control in an active elastic metamaterial with negative capacitance piezoelectric shunting. J. Vib. Acoust. 136, 061008.

Danas, K., Kankanala, S.V., Triantafyllidis, N., 2012. Experiments and modeling of iron-particle-filled magnetorheological elastomers. J. Mech. Phys. Solids 60, 120–138.

Fleury, R., Sounas, D.L., Sieck, C.F., Haberman, M.R., 2014. Sound isolation and giant linear nonreciprocity in a compact acoustic circulator. Science (80-.). 343, 516–519.

Greenleaf, A., Lassas, M., Uhlmann, G., 2003. Anisotropic conductivities that cannot be detected by EIT. Physiol. Meas. 24, 413-419.

Greenleaf, A., Lassas, M., Uhlmann, G., 2003. On nonuniqueness for Calderón's inverse problem. Math. Res. Lett. 10, 685-693.

Gump, J., Finkler, I., Xia, H., Sooryakumar, R., Bresser, W.J., Boolchand, P., 2004. Light-induced giant softening of network glasses observed near the mean-field rigidity transition. Phys. Rev. Lett. 92, 245501.

Hessel, A., Oliner, A.A., 1961. Wave propagation in a medium with a progressive sinusoidal disturbance. IRE Trans. Microw. Theory Tech. 9, 337–343.

Leonhardt, U., 2006. Optical conformal mapping. Science 312, 1777–1780.

Liang, B., Yuan, B., Cheng, J.C., 2009. Acoustic diode: rectification of acoustic energy flux in one-dimensional systems. Phys. Rev. Lett. 103, 1-4.

Liu, X.N., Hu, G.K., Huang, G.L., Sun, C.T., 2011. An elastic metamaterial with simultaneously negative mass density and bulk modulus. Appl. Phys. Lett. 98, 1–3.

Liu, X.N., Huang, G.L., Hu, G.K., 2012. Chiral effect in plane isotropic micropolar elasticity and its application to chiral lattices. J. Mech. Phys. Solids 60, 1907–1921.

Lurie, K.A., 2007. An introduction to the mathematical theory of waves, 3. Springer, New York, NY.

Milton, G.W., 2007. New metamaterials with macroscopic behavior outside that of continuum elastodynamics. New J. Phys. 9, 359.

Milton, G.W., Briane, M., Willis, J.R., 2006. On cloaking for elasticity and physical equations with a transformation invariant form. New J. Phys. 8, 248-267.

Mousavi, S.H., Khanikaev, A.B., Wang, Z., 2015. Topologically protected elastic waves in phononic metamaterials.. Nat. Commun. 6, 8682.

Nassar, H., He, Q.-C., Auffray, N., 2015. Willis elastodynamic homogenization theory revisited for periodic media. J. Mech. Phys. Solids 77, 158–178.

Nassar, H., He, Q.-C., Auffray, N., 2016. On asymptotic elastodynamic homogenization approaches for periodic media. J. Mech. Phys. Solids 88, 274–290.

Nemat-Nasser, S., Srivastava, A., 2011. Overall dynamic constitutive relations of layered elastic composites. J. Mech. Phys. Solids 59, 1953-1965.

Norris, A.N., Shuvalov, A.L., Kutsenko, A.A., 2012. Analytical formulation of three-dimensional dynamic homogenization for periodic elastic systems. Proc. R. Soc. London A Math. Phys. Eng. Sci. 468, 1629–1651.

Pease, M.C., 1965. Methods of Matrix Algebra. Academic Press, New York.

Pendry, J.B., Schurig, D., Smith, D.R., 2006. Controlling electromagnetic fields. Science 312, 1780–1782.

Reed, E.J., Soljačić, M., Joannopoulos, J.D., 2003. Reversed doppler effect in photonic crystals. Phys. Rev. Lett. 91, 89-92.

Sanchez-Palencia, E., 1980. Non-Homogeneous Media and Vibration Theory. Springer-Verlag.

Shuvalov, A.L., Kutsenko, A.A., Norris, A.N., Poncelet, O., 2011. Effective Willis constitutive equations for periodically stratified anisotropic elastic media. Proc. R. Soc. London A Math. Phys. Eng. Sci. 467, 1749–1769.

Simon, J.-C., 1960. Action of a progressive disturbance on a guided electromagnetic wave. IRE Trans. Microw. Theory Tech. 8, 18-29.

Slater, J.C., 1958. Interaction of waves in crystals. Rev. Mod. Phys. 30, 197-222.

Swinteck, N., Matsuo, S., Runge, K., Vasseur, J.O., Lucas, P., Deymier, P.a., 2015. Bulk elastic waves with unidirectional backscattering-immune topological states in a time-dependent superlattice. J. Appl. Phys. 118, 063103.

Torrent, D., Pennec, Y., Djafari-Rouhani, B., 2015. Resonant and nonlocal properties of phononic metasolids. Phys. Rev. B 92, 174110.

Trainiti, G., Ruzzene, M., 2016. Non-reciprocal elastic wave propagation in spatiotemporal periodic structures. New J. Phys. 18, 083047.

Willis, J.R., 1980. A polarization approach to the scattering of elastic waves-I. Scattering by a single inclusion. J. Mech. Phys. Solids 28, 287–305.

Willis, J.R., 1980. A polarization approach to the scattering of elastic waves-II. Multiple scattering. J. Mech. Phys. Solids 28, 307–327. Willis, J.R., 1997. Dynamics of composites. In: Suquet, P. (Ed.), Contin. Micromechanics. Springer-Verlag, New York, Inc., pp. 265–290.

Willis, J.R., 2012. The construction of effective relations for waves in a composite. Comptes Rendus Mécanique 340, 181–192.

Yu, Z., Fan, S., 2009. Complete optical isolation created by indirect interband photonic transitions. Nat. Photonics 3, 91-94.

Zanjani, M.B., Davoyan, A.R., Engheta, N., Lukes, J.R., 2015. NEMS with broken t symmetry: graphene based unidirectional acoustic transmission lines. Sci. Rep. 5, 09926.

Zanjani, M.B., Davoyan, A.R., Mahmoud, A.M., Engheta, N., Lukes, J.R., 2014. One-way phonon isolation in acoustic waveguides. Appl. Phys. Lett. 104. Zaoui, A., 2002. Continuum micromechanics: survey. J. Eng. Mech. 128, 808–816.